IOP Conference Series: Earth and Environmental Science

PAPER • OPEN ACCESS

Fatigue Damage of RC Beams Subjected to Low Level of Fatigue Loading

To cite this article: Shuai Wang *et al* 2019 *IOP Conf. Ser.: Earth Environ. Sci.* **283** 012026

Fatigue Damage of RC Beams Subjected to Low Level of Fatigue Loading

Shuai Wang[1], Jieqiong Wu[1] and Yinghua Ye[1,2]

1. School of Transportation Science and Engineering, Beihang University, Beijing, P.R. China.
2. State Laboratory of Subtropical Building Science, South China University of Technology, Guangzhou, P.R. China.
Email: wangshuai_buaa@163.com

Abstract. The fatigue damage of reinforced concrete (RC) beam specimens subjected to low load level with the upper limit of 0.3Pu, 0.4Pu or 0.5Pu and the lower limit of 0.06Pu were experimentally studied, where Pu was the static ultimate strength of the RC beams. Based on the testing results of concrete strain and mid-span deflection, the effects of load level and fatigue cycle on the accumulation of fatigue damage were discussed. Results show that, the concrete strain, mid-span deflection and residual deflection would undergo a rapid increase followed by a stable change and they all increase as the upper limit or fatigue cycle increased, which indicated that the fatigue damage accumulated as the upper limit or fatigue cycle increased. The steady develop range of concrete strain and deflection became narrow as the upper limit of fatigue load increased to 0.5Pu. Besides, the residual deformation of RC beam specimens showed the boundary of fatigue cycles for steady development was 0.1 million for all load levels of 0.3, 0.4 and 0.5.
Keywords: Fatigue damage; RC beams; Concrete strain; Mid-span deflection; Residual deformation.

1. Introduction

The Reinforced concrete structures in coastal areas or the northern cold region which often use de-icing salt are often affected by external chlorine ion, especially for the structures that bearing repeated or fatigue loads, such as cross-sea bridges, tunnels, coastal railway sleepers, wharfs, and gravity offshore platforms [1]. Not only the carrying capacity of the structures, but also the service life would decrease owing to the combined influence of chlorine ion penetration and fatigue load [2].

In the past few decades, various researches have been carried out to investigate the fatigue problem. Byung [3] experimentally and theoretically studied the fatigue strength of plain concrete subjected to flexural load, and the maximum cyclic stress was changed from almost 0.5 to 1.0 times of the static modulus-of-rupture of concrete. The test data illustrated that under a given stress level, the distribution of fatigue life of plain concrete approximately followed the Weibull probability law. Medeiros et al. [4] conducted the experiment about the effect of loading frequency on the compressive fatigue behavior of plain and fiber reinforced concrete where the maximum stress was 0.85 of its compressive strength. It was found that the fatigue life would become longer at higher frequency. Four-point bending fatigue test was applied under stress level of 0.70 to investigate the fatigue behavior of concrete with water-soluble polymers in the study of Chen et al. [5]. Liu et al. [6] discussed the structural behavior of fatigue damaged reinforced concrete after exposed to corrosion environment. Low load level was adopted with fatigue load level of 0.2 or 0.3 and the number of fatigue cycles was 200,000. The testing results indicated that the residual yielding strength and ultimate strength of these beams reduced as the fatigue load level increased.

During the process of fatigue tests, the accumulation of fatigue damage in RC structures was characterized by the variation of some important parameters, e.g. deflection, stiffness or strain. Raithby [7] experimentally studied the influence factor of the flexural fatigue behavior of plain concrete in which the ratio of maximum cyclic stress and flexural strength ranging from about 0.35 to 1.0. It was highlighted that a general decrease in stiffness was observed towards the end of fatigue life and the tensile strain exceeded about 200 micro-strain when the specimens failed. Fangping Liu and Jianting Zhou [8] comprehensively analyzed the changes of RC beams' strain and stiffness under fatigue loading whose maximum stress level were varied from 0.6 to 0.7. The strain increased by three phases while stiffness degradation of the beam showed a more obvious monotonic decreasing "S" curve.

Furthermore, fatigue damage accumulation could be represented by the depth of the neutral axis varied with fatigue load cycles, which also represented the fatigue damage of concrete. Malumbela et al. [9] monitored the longitudinal tensile and compressive strains during corrosion process under sustain load to discuss the variation of the depth of the neutral axis. However, the study of the development of neutral axis during the fatigue test is lacking in existing literature.

Most of the existing researches focused on the fatigue behavior of materials, such as steel bar or plain concrete. There are few fatigue tests for RC beams, and researchers always choose high level fatigue load to accelerate the experiment progress. For the RC structures, such as RC bridges, their normal service conditions are usually in a relatively low level for fatigue load [8] and the study of RC structures under low level fatigue load is fewer. In addition, detailed data about the variation of strain, deflection, depth of neutral axis and the residual deformation during the fatigue tests were less recorded.

The normal working conditions of reinforced concrete beams were simulated in the lab. Under the fatigue load level of 0.3, 0.4 and 0.5, damage accumulation of specimens in circulation from 400,000 to 4 million times was recorded respectively, including the development of mid-span displacement, strain accumulation, residual deformation accumulation and the variation of neutral axis position. The data collected in this paper was analyzed to provide theoretical basis for safety diagnosis and life prediction of reinforced concrete structures in coastal areas.

2. Experimental Details

2.1. Specimens

Seven RC beam specimens, named as A1 to A3 and B1 to B4, with same sizes and same reinforcements were made from one batch of concrete. Specimens of A1 to A3 were subjected to static loading and B1 to B4 were subjected to fatigue loading. The reinforcement arrangements and geometry dimensions of RC beam specimens are showed in Figure 1. The rectangular cross-section was 150mm×250mm and the length of the beam was 1800mm. The concrete cover was 40 mm and four steel bars with 14 mm diameter were symmetrically placed as longitudinal bars where there was no longitudinal bars in the compression part of the specimen's pure bending zone whose length is 400mm. The proportion of concrete mixtures is listed in Table 1. The compression strength of concrete used for RC beam specimens was 43.0 MPa at loading test.

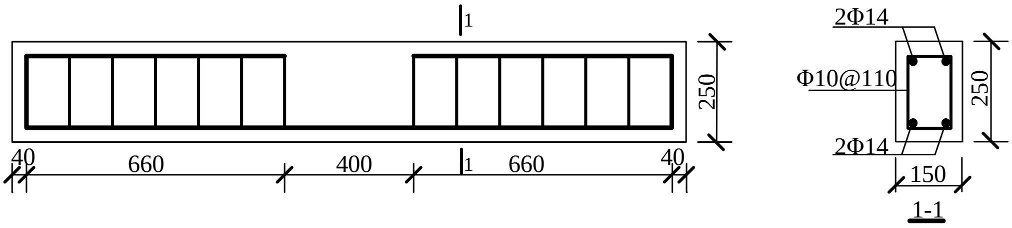

Figure 1. Reinforcement and size of RC beams.

Table 1. Proportions of concrete mixtures.

Mixtures of concrete	Water (kg/m^3)	Portland cement (P.O. 42.5) (kg/m^3)	Coarse aggregates (kg/m^3)	River sand (kg/m^3)	Antifreeze additive (kg/m^3)
	156	381	1020	788	7.9

2.2. Testing Program

All tests were done in the Civil Engineering Laboratory at Beihang University in Beijing. It is well known that the fatigue strength was strongly influenced by the age of concrete and hygrometric conditions during the tests [10], so static loading was applied on A1-A3 to get the ultimate strength at the same age of 365d and B1-B4 were subjected to fatigue loading at the age of 390-405d as shown in Figure 2 and its specific parameters were plotted in Figure 3. The static ultimate strength of A1 to A3 was 105kN, 114kN and 111kN respectively, and the average value of these three numbers is the Pu (110kN). The 0.4 million cycles of fatigue load, where the lower limit was 0.06Pu and the upper limit was 0.3Pu, 0.4Pu and 0.5Pu, were applied on B1, B2 and B3 respectively. And B4 was subject to the 4 million cycles of fatigue load where the lower limit was 0.06Pu and the upper limit was 0.4Pu. Experimental parameters of specimens are given in Table 2. Besides, the frequency of fatigue loading was 5Hz.

Linear Variable Differential Transformer (LVDT), named as L1, was placed on the mid-segment of beam specimens to measure the lateral deformation of concrete with spacing of 300mm and the distance to the upper surface of the beam was 250mm, as shown in Figure 3. Also, the concrete strains in mid-segment were tested in order to investigate the variation of concrete strain in fatigue process. As shown in Figure 3, three strain gauge were arranged above the LVDT, named as T1, T2 and T3. The strain gauge was utilized to measure longitudinal strain of RC beams. Besides, the Deflection Meter was places at the mid- span of the beam specimens to monitor the variation of mid-span deflection.

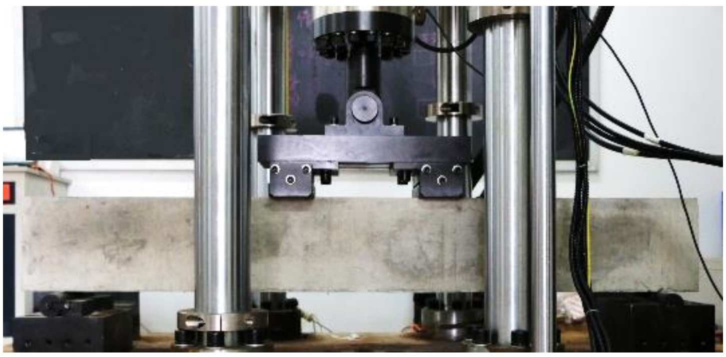

Figure 2. Diagram under fatigue loading.

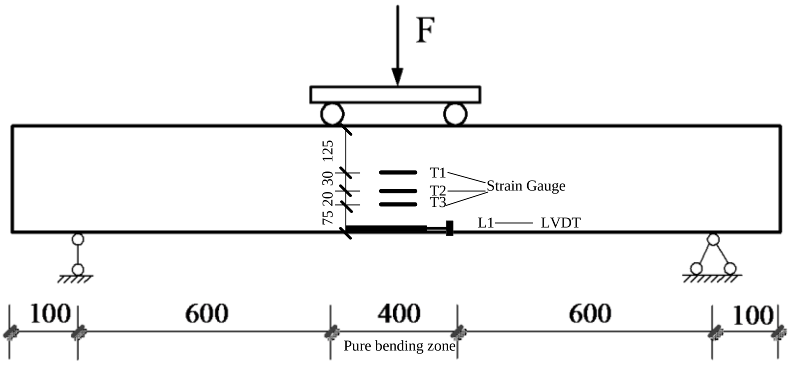

Figure 3. Fatigue loading diagram with arrangement of strain gauge and LVDT.

Table 2. Experimental parameters of RC beam specimens.

Group		Loading Age (d)	Static Load (kN)	Cycles of Fatigue load	Lower limit of Fatigue load	Upper limit of Fatigue load
A	A1	365	105	—	—	—
	A2	365	114	—	—	—
	A3	365	111	—	—	—
B	B1	390	—	0.4 million	0.06Pu	0.3Pu
	B2	395	—	0.4 million	0.06Pu	0.4Pu
	B3	400	—	0.4 million	0.06Pu	0.5Pu
	B4	405	—	4 million	0.06Pu	0.4Pu

Note: Pu is the ultimate strength of RC beam specimens under static load (Pu=110kN).

3. Results and Discussions

3.1. Fatigue Damage of RC Beams

3.1.1. Concrete Strain at Mid-segment of Beam Specimens The tensile concrete strain at point T2 as shown in Figure 3 of B1, B2 and B3 are plotted in Figure 4a, and tensile concrete strain at point T1, T2 and T3 as shown in Figure 3 of B4 are plotted in Figure 4b.

As can be seen from Figure 4a, on one hand, load level had significant impact on the concrete strain since the value of concrete strain in B3 that subject to 0.5Pu of fatigue load was obviously larger than that in B1 and B2 with 0.3Pu and 0.4Pu of fatigue load, respectively. For example, concrete strain in B3 was almost 4.91times of concrete strain in B2 and 8.94 times of concrete strain in B1 when the fatigue cycle was 0.4 million. On the other hand, when the fatigue cycle was about 0.1 million, the variation of concrete strain in B3 was changed from elastic to almost stable, which indicated that the development of concrete strain at point T2 was changed from elasticity to steady as a result of cracks propagation. But the variation of concrete strain in B1 and B2 still showed continual growth until 0.4 million cycles. And due to the specimens B2 and B4 subjected to the same load level, it can be concluded in Figure 4b that for load level of 0.4, concrete strain at point T2 begun its stable phase when the fatigue cycle was almost 1.3 million. Therefore, it can be concluded that tensile concrete strain in B3 developed much faster than B1 and B2 to begin its stable phase, i.e. the boundary of fatigue cycles for stable development of tensile concrete strains would be shortened by the increase of load level and this phenomenon was consistence with the development of crack propagation.

Besides, Figure 4b also showed that in tension zone, concrete strain increased and its growth rate also increased as the distance from the neutral axis increased from 3mm to 5mm where strain increased to 1057με at point T2 and increased to 1334με at point T3. Meanwhile, point T1 was at the center of the cross section that the position of the initial neutral axis and the concrete strain at point T1 gradually increased from 0 to almost 350με, which indicated that the depth of neutral axis or the depth of compression zone decreased as fatigue cycle increased.

Therefore, higher load level contributed to higher tensile concrete strain and faster strain growth rate than lower load level, i.e. more severe damage was produced as load level increased. The variation of concrete strain subjected to higher load level presented stable development earlier than that subjected to lower load level. Concrete strain obviously increased and its growth rate was also raised as the distance from the neutral axis increased, and the depth of neutral axis declined as the fatigue cycle increased.

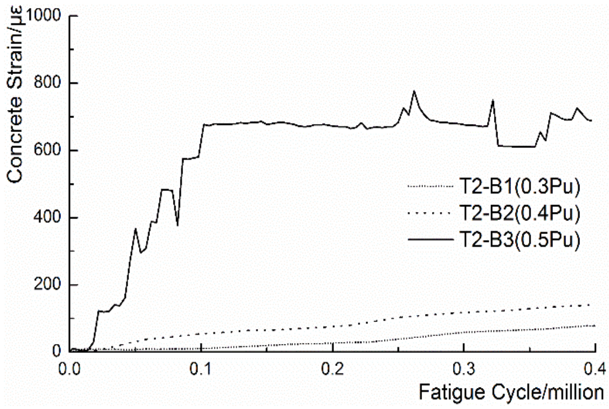

(a) Concrete strain at point T2 in B1, B2 and B3

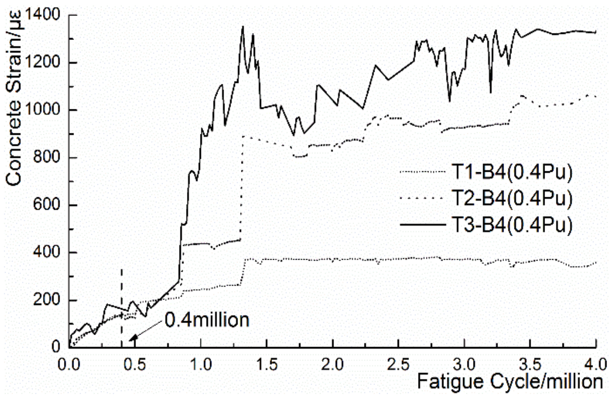

(b) Concrete strain at point T1, T2 and T3 in B4

Figure 4. Variation of concrete strain of beam specimens versus fatigue cycle.

3.1.2. Mid-span Deflection of Beam Specimens Figure 5 gives the development of mid-span deflection in B1 to B4 varied with the fatigue cycle where Figure 5(a) shows the development of mid-span deflection in B1, B2 and B3 as the fatigue cycle increased to 0.4 million, and Figure 5(b) shows the development of mid-span deflection in B4 with load level of 0.4 as the fatigue cycle increased to 4 million. Generally, mid-span deflection of all beam specimens underwent an elastically growth followed by a steady growth period as fatigue cycle increased.

As can be seen from Figure 5a, the deflection of B2 with 0.4 load level was significantly smaller than that of B3 with 0.5 load level and obviously larger than that of B1 with 0.3 load level, but the gap among the deflection of B1, B2 and B3 was almost the same. It is worth mentioning the deflection of B1, B2 and B3 elastically increased to 1.12mm, 1.54mm and 2.01mm respectively at around 0.007 million cycles. And in the next 3.993 million cycles, the deflection of B1 gradually increased from 1.12mm to 1.64mm and B2 gradually increased from 1.54mm to 2.10mm as well as deflection of B3 steadily increased from 2.01mm to 2.89mm. This illustrated that the variation of mid-span deflection of beam specimens that subject to different load levels showed similar boundary of fatigue cycles for stable development, which was different from the variation of cracks and concrete strain that the boundary of fatigue cycles for stable development would decrease as load level increased to 0.5. Figure 5(b) shown the same tendency as the fatigue cycles increased from 0 to 4 million for B4.

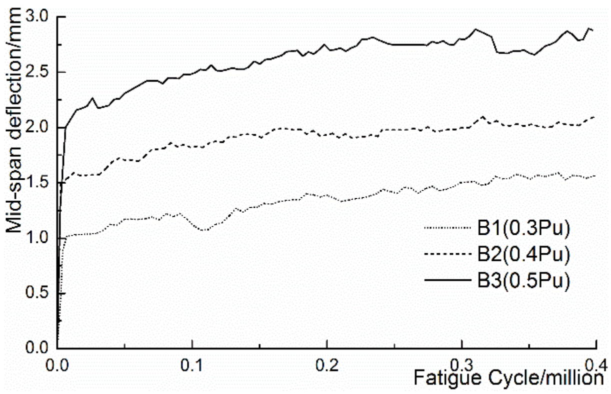

(a) Mid-span deflection in B1 B2 and B3

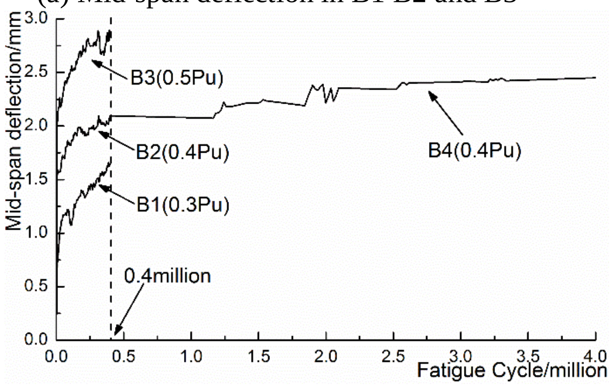

(b) Mid-span deflection in B4

Figure 5. Variation of mid-span deflection of beam specimens versus fatigue cycle.

3.1.3. Residual Deformation of Beam Specimens. In the previous study of Park [11], residual strain was highlighted to represent the accumulation of fatigue damage. Therefore, residual deformation including the residual mid-span deflection of beam specimens and residual strain of tensile concrete were analyzed here to characterize damage accumulation based on the theory that the variation of the residual deformation can be utilized to trace a fatigue process. The variation of residual mid-span deflection in B1, B2 and B3 as fatigue cycle increased to 0.4 million was plotted in Figure 6(a) and residual strain at point L1 in B2 and B3was given in Figure 6(b), respectively. Since the connection between the data acquisition instrument and LVDT in B1was broken, the residual strain at point L1 in B1 was not obtained. It was concluded in Figure 6 that although B1, B2 and B3 were subject to different load levels (0.3, 0.4 and 0.5), the residual deformation of these there beam specimens shared similar variation that a rapid growth followed by a stable development. For example, when the fatigue cycle was about 0.1million, residual deflection in mid-span of B1, B2 and B3 rapidly increased to 0.81mm, 0.97mm and 1.0mm respectively and then they all showed a stable increase in the next 0.3 million cycles. And it was also concluded that the value of the residual deformation of B3 with 0.5 load level and that of B2 with 0.4 load level was similar but the value of B1 with 0.3 load level was a little smaller than that of B2 and B3. Similarly, the residual strain of tensile concrete at L1 in B2 and B3 jumped to around 1000με at first 0.01million cycles before a stable development was presented in the following fatigue cycles. Besides, by comparing the variation of residual deformation in Figure 6

(a) and (b), it was found that the accumulation of residual deflection in mid-span lagged behind the accumulation of residual strain in tensile concrete. A possible explanation was that the residual strain at L1 represent the damage accumulation in local RC beam specimens (tensile concrete) while the residual deflection in mid-span characterized the integral deformation of RC beam specimens which was contributed to the damage accumulation of local specimens.

Furthermore, Figure 7 gives the variation of residual mid-span deflection in B4 as fatigue cycle increased to 4 million. It was clearly illustrated that during the long period of fatigue test, residual deflection tended to grow sharply at first 0.1 million cycles and then the growth rate gradually decreased as fatigue cycle increased to 4 million, which was consistence with the conclusion of Figure 6(a).

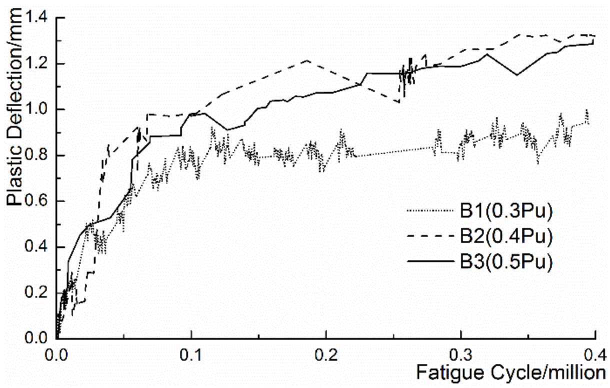

(a) Residual defection in B1, B2 and B3

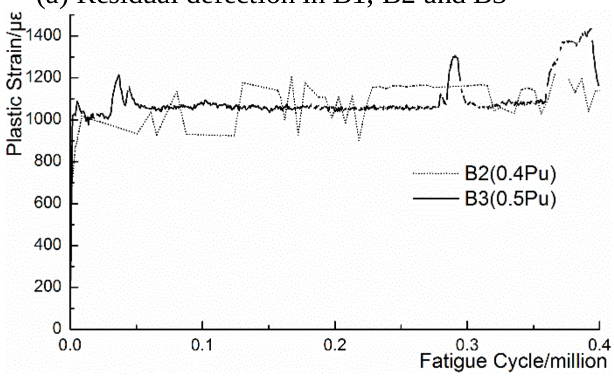

(b) Residual strain in B2 and B3 at L1

Figure 6. Variation of residual deformation of beam specimens versus fatigue cycle.

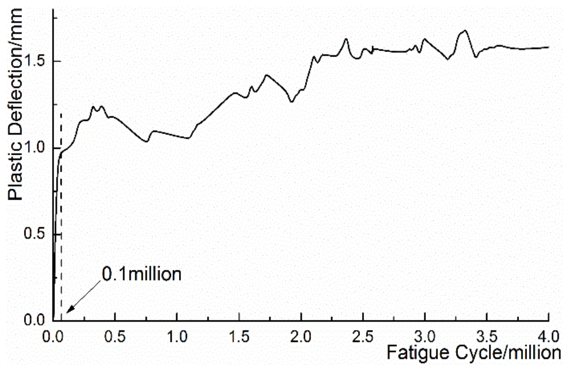

Figure 7. Variation of residual deflection of beam specimens versus fatigue cycle (B4).

3.1.4. Depth of Neutral Axis The depth of the neutral axis at the mid-span section of beam specimen was calculated from measured strains by assuming that the average tensile strains were linearly related to compressive strains resulting from the model deflections of cracked RC members [12-13]. Figure 8 shows the variation of the depth of neutral axis in B4 with 0.4 load level as the fatigue cycle increased to 4.0 million. As expected from the variations of concrete strains in Section 3.1.1, the depth of the neutral axis of B4 generally declined. To be more specific, the depth of neutral axis steadily developed at first 1.5 million cycles and then rapidly decreased to about 10mm in the following 0.2 million cycles before fluctuated around 10mm as fatigue cycle increased to 4.0 million. This variation can be attributed to the propagation of flexural cracks and the development of concrete strains as shown in Section 3.1. Additionally, the depth of neutral decreased or the depth of compression zone declined also represented the accumulation of fatigue damage.

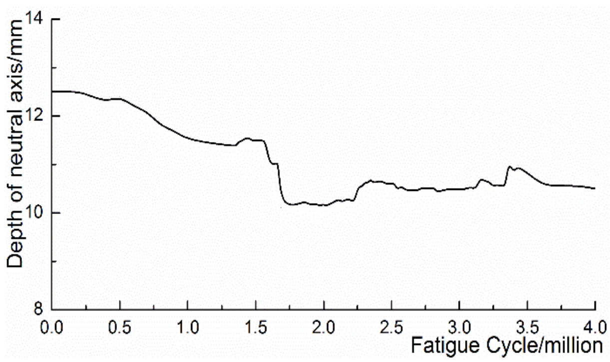

Figure 8. Variation of depth of neutral axis in B4 versus fatigue cycle.

4. Conclusions

To simulate the normal working conditions of RC beams for bridges in coastal areas, low level (0.3\0.4\0.5) fatigue load was brought to bear on beam specimens with different fatigue cycle times (0.4million\4million). The fatigue damage of concrete and RC beam specimens were studied by the variation of concrete strain, mid-span deflection, residual deformation and the depth of neutral axis as fatigue cycle or load level increased. Conclusions specifically are as follows:

(1) The fatigue damage accumulation under low load level would continually increase from the beginning of the fatigue cycles to the end. The overall trend is rapid growth followed by steady growth. In addition, the range of fatigue cycles for the steady development narrowed as load level increased.

(2) As the load level increased from 0.3 to 0.5, the variation of concrete strain and deflection showed an elastic increase followed by a stable development where the period of elastic change of deflection was similar under load levels of 0.3, 0.4 and 0.5.

(3) The residual deformation of RC beam specimens showed a rapid increase followed by a steady growth and the boundary of fatigue cycles for steady development was 0.1 million for all load levels of 0.3, 0.4 and 0.5.

Acknowledgments

This work was financially supported by the National Natural Science Foundation of China (Grant no. 51578031) and the Open Project of State Key Laboratory of Subtropical Building Science, South China University of Technology (2016ZA03).

References

[1] Skar A, Poulsen P N, Olesen J F. A simple model for fatigue crack growth in concrete applied to a hinge beam model [J]. Engineering Fracture Mechanics, 2017, 181.

[2] Fathima K M P, Kishen J M C. A thermodynamic correlation between damage and fracture as applied to concrete fatigue [J]. Engineering Fracture Mechanics, 2015, 146:1-20.

[3] Byung Hwan Oh. Fatigue Analysis of Plain Concrete in Flexure [J]. Journal of Structural Engneering, 1986, 112 (2):273-288.
[4] Medeiros A, Zhang X, Ruiz G, et al. Effect of the loading frequency on the compressive fatigue behavior of plain and fiber reinforced concrete [J]. International Journal of Fatigue, 2015, 70:342-350.
[5] Chen B, Guo L, Sun W. Fatigue Performance and Multiscale Mechanisms of Concrete Toughened by Polymers and Waste Rubber [J]. Advances in Materials Science & Engineering, 2014, 2014 (4):1-7.
[6] Liu Z, Diao B, Zheng X. Effects of Seawater Corrosion and Freeze-Thaw Cycles on Mechanical Properties of Fatigue Damaged Reinforced Concrete Beams [J]. Advances in Materials Science & Engineering, 2015, 2015 (1):1-15.
[7] Raithby K D. Flexural fatigue behavior of plain concrete [J]. Fatigue of Engineering Materials and Structures, 1979, 2 (3):269-278.
[8] Liu F, Zhou J. Experimental Research on Fatigue Damage of Reinforced Concrete Rectangular Beam[J]. Ksce Journal of Civil Engineering, 2018 (1):1-12.
[9] Malumbela G, Moyo P, Alexander M. Behaviour of RC beams corroded under sustained service loads [J]. Construction & Building Materials, 2009, 23 (11):3346-3351.
[10] Galloway, J W, Raithby K D, Harding H M. Effects of moisture changes on the flexural strength and fatigue performance of concrete [J], Report LR 864, 1979.
[11] Park Y J. Fatigue of Concrete under Random Loadings [J]. Journal of Structural Engineering, 1990, 11 6(11):3228-3235.
[12] El Maaddawy T, Soudki K, Topper T. Analytical model to predict nonlinear flexural behaviour of corroded reinforced concrete beams [J]. ACI Structural Journal 2005;102(4):550-9.
[13] Ghali A, Favre R. Concrete structures: stresses and deformations /-3rd ed [M]. Spon Press, 2002.